

Statistical mechanics guides the motions of cm scale objects

S. Siriroj,¹ P. Simakachorn,^{1,2} N. Khumtong,² T. Sukhonthamethirat,² S. Chaiyachad,^{1,3} P. Chanprakhon,^{1,3} K. Chanthorn,^{1,3} S. Dawprateep,^{1,3} T. Eknapakul,^{1,3} I. Fongkaew,^{1,3} C. Jaisuk,^{1,3} T. Jampreecha,^{1,3} W. Jindata,^{1,3} Y. Kaeokhamchan,^{1,3} T. Kongnok,^{1,3} P. Laohana,^{1,3} K. Lapawer,^{1,3} S. Lowpa,^{1,3} A. Mooltang,^{1,3} S. Musikajaroen,^{1,3} S. Nathabumroong,^{1,3} A. Panpar,^{1,3} S. Phumying,^{1,3} S. Polin,^{1,3} A. Rasritat,^{1,3} A. Ritwiset,^{1,3} W. Saengsui,^{1,3} W. Saenrang,^{1,3} T. Saisopa,^{1,3} S. Sangphet,^{1,3} T. Sawasdee,^{1,3} S. Sonsupap,^{1,3} S. Suksombat,^{1,3} T. Suyuporn,^{1,3} M. Tepakidareekul,^{1,3} T. Thiwatwanikul,^{1,3} P. Tipsawat,^{1,3} S. Waiprasoet,^{1,3} and W. Meevasana^{1,3,*}

¹*School of Physics, Suranaree University of Technology, Nakhon Ratchasima, 30000, Thailand*

²*SCiUS program, Suranaree University of Technology and Rajsima Wittayalai School, Nakhon Ratchasima, 30000, Thailand*

³*Thailand Center of Excellence in Physics, CHE, Bangkok 10400, Thailand*

(Dated: May 29, 2018)

Calculations and mechanistic explanations for the probabilistic movement of objects at the highly relevant cm to m length scales has been lacking and overlooked due to the complexity of current techniques. Predicting the final-configuration probability of flipping cars for example remains extremely challenging. In this paper we introduce new statistical methodologies to solve these challenging macroscopic problems. Boltzmann's principles in statistical mechanics have been well recognized for a century for their usefulness in explaining thermodynamic properties of matter in gas, liquid and solid phases. Studied systems usually involve a large number of particles (e.g. on the order of Avogadro's number) at the atomic and nanometer length scales. However, it is unusual for Boltzmann's principles to be applied to individual objects at centimeter to human-size length scales. In this manuscript, we show that the concept of statistical mechanics still holds for describing the probability of a tossed orthorhombic dice landing on a particular face. For regular dice, the one in six probability that the dice land on each face is well known and easily calculated due to the 6-fold symmetry. In the case of orthorhombic dice, this symmetry is broken and hence we need new tools to predict the probability of landing on each face. Instead of using classical mechanics to calculate the probabilities, which requires tedious computations over a large number of conditions, we propose a new method based on Boltzmann's principles which uses synthetic temperature term. Surprisingly, this approach requires only the dimensions of the thrown object for calculating potential energy as the input, with no other fitting parameters needed. The statistical predictions for landing fit well to experimental data of over fifty-thousand samplings of dice in 23 different dimensions. We believe that the ability to predict, in a simple and tractable manner, the outcomes of macroscopic movement of large scale probabilistic phenomena opens up a new line of approach for explaining many phenomena in the critical centimeter-to-human length scale.

PACS numbers:

Tossing a die from a significant height on a hard floor is generally thought as a random process since its motion is unpredictable from the initial state of the die. However, regardless of its random motion, one can accurately predict that the probability of a die landing on any particular face of a standard cubic die is $1/6$. This predictability is the result of the six-fold symmetry of the die alone. It is non-trivial to ask, "how will this $1/6$ probability change if we break this six-fold symmetry?" The motion of a macroscopic object is in principle governed by classical mechanics and Newton's laws. If all the necessary initial conditions are given, the equations of motion can be written for calculating the coordinates and momenta of an object anytime thereafter. In practice, the bouncing motion of simple objects, e.g. dice and coins, is already difficult to calculate. We are not aware of any previous work studying the motion of a bouncing die using the full die geometry, although the bouncing motion of a simplified object such as a barbell has already been reported by Nagler and Richter [1]. The calculated phase space of the final configuration of

the barbell (i.e. whether the barbell points to the left or right) is already very complex [1]. Furthermore, phase spaces with different parameters for the surrounding environment (e.g. friction coefficients) are computationally intensive to be re-calculated every time when a condition is changed. Note that if no bouncing occurs (e.g. a thick coin landing on a soft-rice bed [2]), the phase space can be calculated; our work looks into a more general case where bouncing is allowed.

Since the classical-mechanics approach is so complex as to be impracticable and computationally intractable, we looked for a simpler method that could utilize statistical principles. The Boltzmann distribution in statistical mechanics attracted our attention as the principle requires only knowing an ensemble of energy states and temperature to determine the distribution in each state of particles. By constructing a partition function based on this Boltzmann factor, $e^{-\epsilon_i/k_B T}$ where ϵ_i is the energy in each state i , and T is temperature, one can predict many thermodynamic properties such as heat capacity of a solid and magnetic susceptibility as a function of tem-

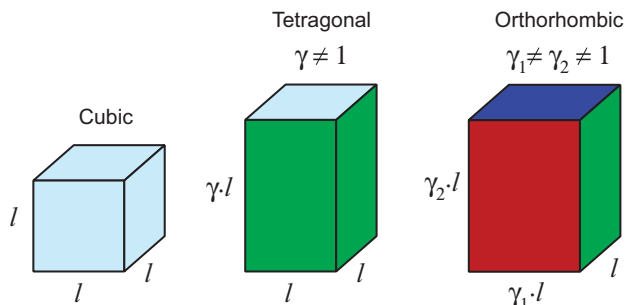


FIG. 1: Geometry of regular dice (left), tetragonal dice (middle) and orthorhombic dice (right). The parameters γ , γ_1 and γ_2 are the ratios between extended/contracted sides and the common length l .

perature [5, 6]. The concepts of statistical mechanics are also useful at large length scales (e.g. star distribution [3], with proposed entropic forces [4]) used for objects such as stars and black holes. In this work, we are interested in applying the Boltzmann concept to a set of tossed dice in 23 different dimensions (see results in Fig. 2). The redefined temperature term, which is important for describing the outcome, is explained in a later section (see eq. (13)).

For experimental measurements, the die shape and parameters are defined as follows: Fig. 1 shows a cubic die with length of each side l . For the tetragonal and orthorhombic dice, γ , γ_1 and γ_2 are dimensionless ratios between extended/contracted sides and the common length l , describing the dimensions of each die. All dice are custom-made from solid aluminum. With l of 0.9 cm, there are 11 sizes of tetragonal dice with varied γ as displayed along x-axis in Fig. 2(a) and 11 sizes of orthorhombic dice with fixed γ_1 of 1.3 and varied γ_2 as displayed along x-axis in Fig. 2(b). For each dimension, we toss the dice around 2400 times on average by dropping them from a height of 27 cm above a leveled and flat floor composed of thick and hard ceramic. Note that the height from which the dice are dropped is many times larger than the dimension of each dice. At this height, random outcomes are expected and the regular die gives a 1/6 measured probability as expected due to symmetry (please see supplementary materials for more explanation [8]). To avoid biased measurements, the 33 persons, who tossed the dice, were not told about the prediction results beforehand.

As shown in Fig. 2(a), we have measured the final configuration probabilities of tossed tetragonal dice by varying the γ factor. The outcome appears to have a well-organized structure for the probability when plotted as a function of the dimensionless length ratio γ . As the die is colored with blue and green on 2 square faces and 4 rectangular faces respectively, the blue region in Fig. 2(a) represents the probability of the blue face being up (called γ state) and vice versa for the green region; for

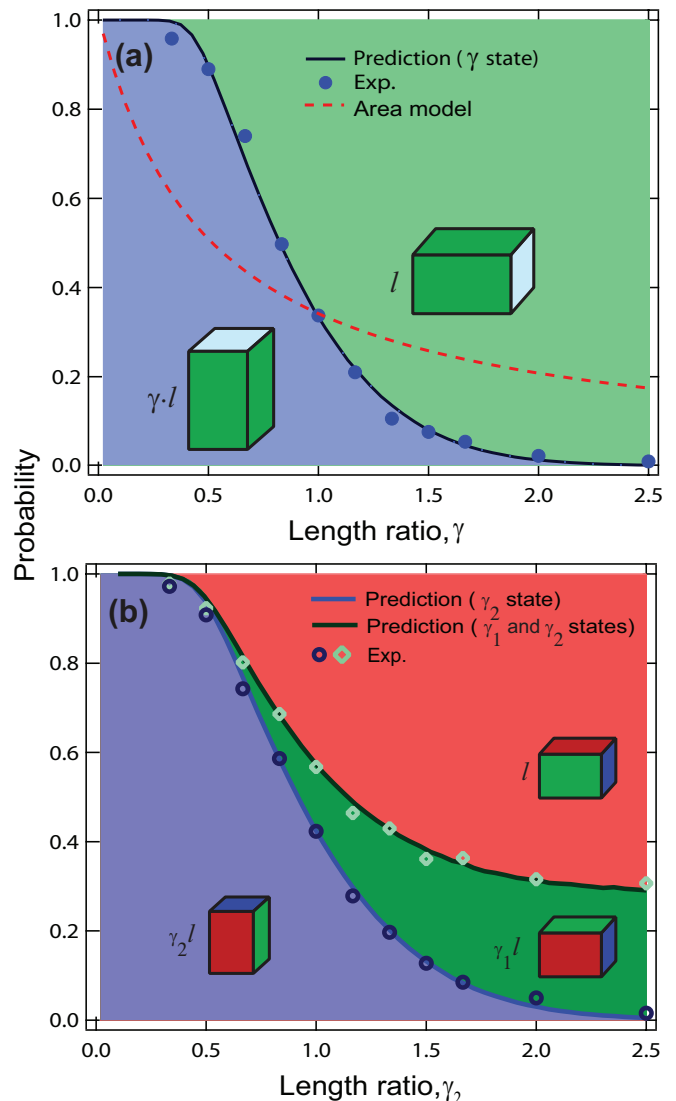


FIG. 2: Probability distribution of landed dice being in different orientations shown in the inset figures for (a) tetragonal dice and (b) orthorhombic dice. The solid lines are model based predictions.

examples, a) if γ is nearly zero (i.e. a thin square sheet), the probability in observing the blue face up should be nearly 1 b) if γ is large (i.e. a long stick with square cross-section), the probability of finding the green face up should also be nearly 1 and c) if γ is exactly one (i.e. a cubic), the probability in landing with a blue(green) face up should theoretically be around 1/3 and 2/3 respectively due to the symmetry. For the orthorhombic dice, the probability outcome as a function of γ_2 is shown in Fig. 2(b). The blue region represents the probability of the blue face being up (the γ_2 state) and the same is applied for the red and green regions.

To model these experimental results, one could simply presume that the probability outcome is directly proportional to the area of the face being up. For exam-

ple, in the case of a tetragonal die with dimension of $1 \times 1 \times 1.5 \text{ cm}^3$ (i.e. $\gamma = 1.5$), the area of blue faces will be $1+1 = 2 \text{ cm}^2$ while the total area of all faces will be $1+1+1.5+1.5+1.5+1.5 = 8 \text{ cm}^2$; hence this area model will predict that the probability of getting blue faces should be $2/8 = 0.25$ while the measured probability is only around 0.076. In Fig. 2(a), this area model for the same range of γ is plotted. This area model is clearly erroneous except for around $\gamma = 0$ and 1.

In this work, a statistical-mechanics approach is chosen and the concept of a Boltzmann distribution is applied. Through rederiving the Boltzmann distribution function we can translate and define the relevant parameters, including energy states and temperature, which are relevant to predicting and understanding our experimental results.

The Boltzmann distribution of a system at equilibrium with a total number of particles $N = \sum_i n_i$ and total energy $E = \sum_i \varepsilon_i n_i$ (for all energy states ε_i) can be derived by maximizing the entropy $S = k \ln W$ [7]. The constraints are that $N = \sum_i n_i = \text{const}$ and $E = \sum_i \varepsilon_i n_i = \text{const}$. Then one will arrive that

$$n_i = e^{-\alpha} e^{-\beta \varepsilon_i} \quad (1)$$

where α and β are constants.

With $N = \sum_i n_i$ and definition of temperature T , we can arrive with

$$n_i = \frac{N}{Z} e^{-\varepsilon_i/kT} \quad (2)$$

where the partition $Z = \sum_i e^{-\varepsilon_i/kT}$. Details of the derivation can be found in the supplementary information [8].

In the continuous case, an average energy $\langle \varepsilon \rangle = \langle \varepsilon(x_i, p_i) \rangle$ [5, 6] can be calculated as:

$$\langle \varepsilon \rangle = \frac{\int \int \varepsilon \cdot e^{-\varepsilon(x_i, p_i)/kT} dx_i dp_i}{\int \int e^{-\varepsilon(x_i, p_i)/kT} dx_i dp_i}. \quad (3)$$

In this way, one can associate the temperature term with the average energy instead of using the formal definition $T \equiv \partial E / \partial S$ which may be harder to use in our case. For example, the average kinetic energy of monatomic gas is:

$$\langle \varepsilon \rangle = \frac{\int \int \int \frac{p_x^2 + p_y^2 + p_z^2}{2m} e^{-\frac{p_x^2 + p_y^2 + p_z^2}{2mkT}} dp_x dp_y dp_z}{\int \int \int e^{-\frac{p_x^2 + p_y^2 + p_z^2}{2mkT}} dp_x dp_y dp_z} = \frac{3}{2} kT \quad (4)$$

where $\varepsilon = (p_x^2 + p_y^2 + p_z^2)/2m$; hence, the temperature term $kT = 2\langle \varepsilon \rangle/3$.

In our case, the total energy of a die, which includes a) translational kinetic energy, b) rotational kinetic energy

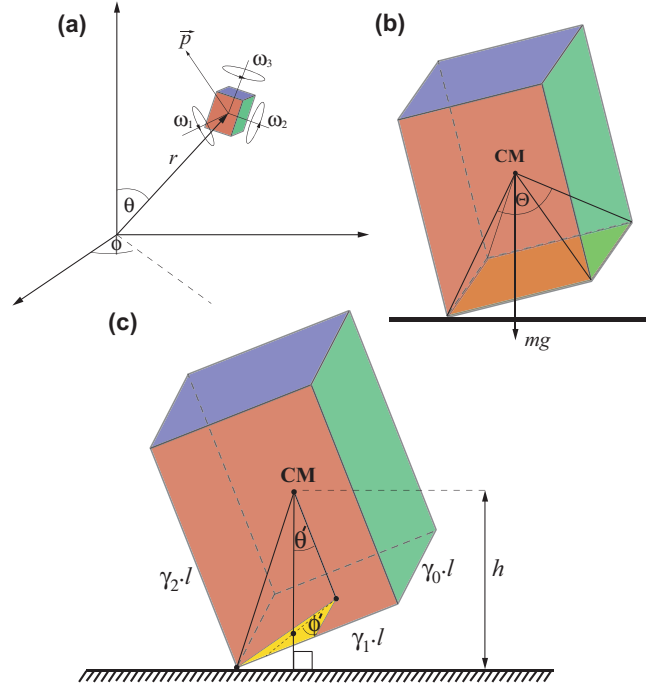


FIG. 3: Schematic diagrams of (a) a die with degrees of freedom for calculating the total energy (eq. (5)), (b) the solid angle where the weight vector points within and the final configuration will end up in γ_2 state, and (c) defined variables for integrations in eq. (8).

and c) potential energy (see Fig. 3(a)), can be written as:

$$\varepsilon_d = \varepsilon(\omega_i, p_i, r, \theta, \phi) = \sum_{i=1}^3 \frac{p_i^2}{2m} + \sum_{j=1}^3 \frac{1}{2} I_j \omega_j^2 + mgr \cos \theta. \quad (5)$$

To avoid confusion with the common temperature, we will replace the term kT by $\kappa\tau$ which will be used as the redefined temperature for large objects from now on. By using eq. (3), the average energy $\langle \varepsilon_d \rangle$ as a function of $\kappa\tau$ can be calculated as:

$$\begin{aligned} \langle \varepsilon_d \rangle &= \frac{\int \int \int \varepsilon(\omega_i, p_i, r, \theta, \phi) \cdot e^{-\varepsilon(\omega_i, p_i, r, \theta, \phi)/\kappa\tau} d^3 p d^3 \omega d^3 r}{\int \int \int e^{-\varepsilon(\omega_i, p_i, r, \theta, \phi)/\kappa\tau} d^3 p d^3 \omega d^3 r} \\ &= 6\kappa\tau. \end{aligned} \quad (6)$$

The average energy can now be written as a function of $\kappa\tau$ (i.e. eq. (6) whose detailed derivation is in Supplemental Material [8]). In general, the $\kappa\tau$ term is arbitrary. However, when a specific condition is given, the $\kappa\tau$ term can be calculated via a self-consistent equation. This is a crucial step. When the orthorhombic dice in Fig. 2(b) were tossed, the total energy of the dice started from the high value and then dissipated until coming to rest in

either blue, green or red configuration. In the case that the dice ended up being in blue region (γ_2 state), potential energy at some point in time (when kinetic energy is zero) must be in the configuration that a die has one corner (or more) touching the floor while the weight vector (mg) points down within the solid angle Θ as shown in Fig. 3(b); then the die may move around some more and eventually dissipates energy until it reaches the γ_2 state. These particular configurations give us the condition to calculate the average energy as follow.

$$\langle \varepsilon_d \rangle_{general} = 6\kappa\tau = \langle \varepsilon_d \rangle_{constrained}. \quad (7)$$

In our case, since the kinetic energy at that moment is zero and one corner touches the floor, we need to integrate only in angular space (θ, ϕ):

$$\langle \varepsilon_d \rangle = 6\kappa\tau = \frac{\int \varepsilon(\theta, \phi) \cdot e^{-\varepsilon(\theta, \phi)/\kappa\tau} d\Theta}{\int e^{-\varepsilon(\theta, \phi)/\kappa\tau} d\Theta}. \quad (8)$$

Instead of using the observer frame, the integral over the triangular solid angle (yellow region) in Fig. 3(c) is done in the object frame (θ, ϕ):

$$\begin{aligned} Ie(\gamma_0, \gamma_1, \gamma_2, \kappa\tau) &= \int \varepsilon \cdot e^{-\varepsilon/\kappa\tau} d\Theta \\ &= \int mg \cdot h(\theta, \phi) \cdot e^{-mgh/\kappa\tau} \sin(\theta) d\theta d\phi \\ Iz(\gamma_0, \gamma_1, \gamma_2, \kappa\tau) &= \int e^{-\varepsilon/\kappa\tau} d\Theta \\ &= \int e^{-mgh/\kappa\tau} \sin(\theta) d\theta d\phi \end{aligned} \quad (9)$$

where

$$\phi \in \{0, \tan^{-1}(\gamma_1/\gamma_0)\}, \quad (10)$$

$$\theta \in \{0, \tan^{-1}(\gamma_0/\gamma_2 \cos \phi)\}, \quad (11)$$

$$h = \frac{l}{2}(\gamma_0 \sin \theta \cos \phi + \gamma_1 \sin \theta \sin \phi + \gamma_2 \cos \theta) \quad (12)$$

whose detailed derivations can be read from Ref. [8].

To calculate the average energy, we need to integrate all the 6 faces of the die. This can be calculated using eqs. (8)-(11) where the parameters γ_0, γ_1 and γ_2 can be swapped for the integration on each face (e.g. the yellow triangle in Fig. 3(c)) and for each configuration of γ_0, γ_1 and γ_2 , there are 8 equivalent pieces on the die surface. By summing Ie and Iz for all configurations, covering all the die surface, the eq. (7) can be written as:

$$\langle \varepsilon_d(\kappa\tau) \rangle = \frac{\sum_{i \neq j \neq k} 8Ie(\gamma_i, \gamma_j, \gamma_k, \kappa\tau)}{\sum_{i \neq j \neq k} 8Iz(\gamma_i, \gamma_j, \gamma_k, \kappa\tau)} = 6\kappa\tau \quad (13)$$

where each index runs from 0 to 2.

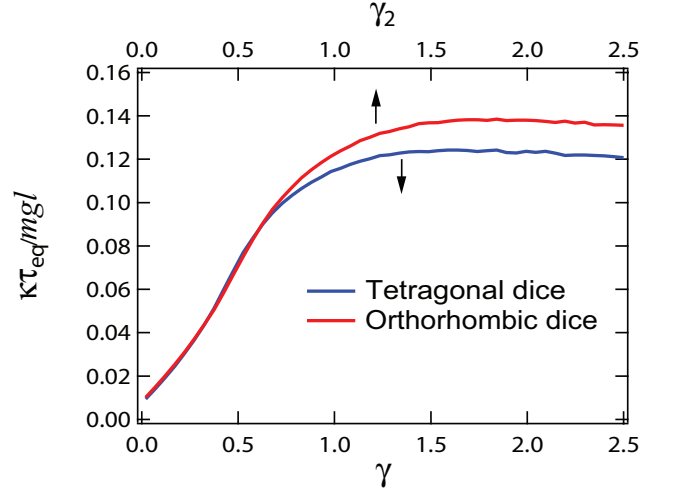


FIG. 4: Temperature

From this eq. (12), the $\kappa\tau_{eq}$ for each γ_2 of the orthorhombic dice can be calculated numerically as shown in Fig. 4. And by plugging in these calculated temperature terms $\kappa\tau_{eq}$, the probability in getting blue, green or red face of the orthorhombic dice is given by:

$$\begin{aligned} P_{orth,blue} &= \frac{Iz(\gamma_0, \gamma_1, \gamma_2, \kappa\tau_{eq}) + Iz(\gamma_1, \gamma_0, \gamma_2, \kappa\tau_{eq})}{Z_{orth}} \\ P_{orth,green} &= \frac{Iz(\gamma_0, \gamma_2, \gamma_1, \kappa\tau_{eq}) + Iz(\gamma_2, \gamma_0, \gamma_1, \kappa\tau_{eq})}{Z_{orth}} \\ P_{orth,red} &= \frac{Iz(\gamma_1, \gamma_2, \gamma_0, \kappa\tau_{eq}) + Iz(\gamma_2, \gamma_1, \gamma_0, \kappa\tau_{eq})}{Z_{orth}} \end{aligned} \quad (14)$$

where $Z_{orth} = \sum_{i \neq j \neq k} Iz(\gamma_i, \gamma_j, \gamma_k, \kappa\tau_{eq})$, $\gamma_0 = 1$ and $\gamma_1 = 1.3$.

For the tetragonal dice, the calculations are the same as the case of the orthorhombic dice except setting $\gamma_0 = \gamma_1 = 1$. The temperature term for the tetragonal dice is also plotted in Fig. 4. It should be emphasized that the normalized temperature term $\kappa\tau_{eq}/mgl$ only depends on the shape (i.e. dimensionless γ terms) but not the mass and the length. Hence eq. (13) will give the same result of probability for the object with the same shape regardless of its size. This is consistent with the classical mechanics where the final configuration should not depend on mass or length of the object (e.g. a freely-falling object always accelerates at g).

Finally, the predictions from eq.(13) are calculated by using the $\kappa\tau_{eq}/mgl$ shown in Fig. 4. The predictions are then plotted in Fig. 2(a) and 2(b). The comparison with the experimental measurements shows excellent agreement with coefficients of determination (R^2): 0.996 for γ state in Fig. 2(a), 0.997 and 0.995 for γ_2 and $\gamma_1 + \gamma_2$ state in Fig. 2(b) respectively.

With the statistical approach providing for high accu-

racy predictions, it could open the door to many applications. Without having to resort to calculating ensembles of full trajectories, the Boltzmann formalism with redefined temperature can be used as a simple and tractable method for explaining and understanding the probability distribution of the final configuration of moving macroscopic objects which eventually come to rest, e.g. saving the cost of computation and experimental testing. This method may also find application to the packing problems [9–12]. By pouring objects into a container (without shaking), the packing factor may be difficult to calculate without knowing the probability of each object landing in a particular configuration.

We would like to thank Ben Segal, Jan Zaanen and David Ando for the ideas initiating this work and suggestions. This work was supported by Thailand Research Fund (TRF) and Suranaree University of Technology (SUT) (Grant No. BRG5880010) and Research Fund for DPST Graduate with First Placement (Grant No. 021/2555). S.Siroj acknowledges the Royal Golden Jubilee Ph.D. Program (Grant no. PHD/0007/2555).

- [1] J. Nagler and P. Richter, *Phys. Rev. E.* 78, 036207 (2008).
- [2] E.H. Yong and L. Mahadevan, *Am. J. Phys.* 79, 1195 (2011).
- [3] J. N. Bahcall and R. A. Wolf. *Astron. J.* 209, 214-232 (1976)
- [4] E. Verlinde, *J. High Energy Phys.* 1104, 29 (2011).
- [5] R. K. Pathria, "Statistical mechanics," Butterworth Heinemann, Oxford, UK, 1972.
- [6] D. L. Goodstein, *States of Matter*, Prentice-Hall, Englewood Cliffs, NJ, 1975.
- [7] Derivation of Boltzmann distribution is from the lecture note of Prof. Angel C de Dios; Also, H. A. Bent, "The Second Law," Oxford University Press, New York, 1965.
- [8] See Supplemental Material at [URL] for probability as a function of dropping height and mathematical derivations.
- [9] A. Donev, F. H. Stillinger, P. M. Chaikin and S. Torquato, *Phys. Rev. Lett.* 92, 255506 (2004)
- [10] A. Donev, I. Cisse, D. Sachs, E. A. Variano, F. H. Stillinger, R. Connelly, S. Torquato, P. M. Chaikin, *Science* 303, 990993 (2004)
- [11] A. Jaoshvili, A. Esakia, M. Porrati and P. M. Chaikin, *Phys. Rev. Lett.* 104, 185501 (2010)
- [12] C. Zong, *Expo. Math.* 32, 297364 (2014)

* Authors to whom correspondence should be addressed.
Electronic addresses: worawat@g.sut.ac.th